Journal of Southeast University (English Edition) Vol. 42, No. 2, pp. 198-205 June 2026 ISSN 1003-7985

Improved inversion of highway traffic loads by eliminating usual environmental microvibrations

XING Yunlin[1], ZENG Xianhong[2], WU Han[3], LOU Yu[1]

(1. China Electronics Engineering Design Institute, Beijing 100142, China; 2. School of Rail Transportation, Wuyi University, Jiangmen 529020, China; 3. Institute of Mechanics, Chinese Academy of Sciences, Beijing 100190, China)

Abstract: Usual environmental microvibrations (UEMs) can introduce inaccuracies for field-measured traffic-induced vibration responses, leading to significant errors in the inversion of highway traffic loads. This study proposed a method for eliminating UEMs in combination with the inverse pseudoexcitation method to invert highway traffic loads. The real vibration response caused by traffic loads was obtained by separating the UEM component from the measured ground vibration response of a site through a frequency-domain transformation. The frequency response function was subsequently derived using finite element simulation technology. Finally, the traffic load spectrum was inversely identified by performing a matrix inversion operation on the frequency response function matrix. The vibration response at a measurement point was calculated using the inverted traffic load spectrum from a synchrotron radiation light source project and compared with field measurements. The relative error decreased from 21.15% to 6.82%, validating the effectiveness of the proposed method. This approach avoided a complex vehicle-road coupling analysis and provided a reliable technical means for load inversion at sites sensitive to microvibration.

Key words: inverse pseudoexcitation method; usual environmental microvibrations (UEMs); highway traffic loads; microvibration-sensitive sites

DOI: 10.3969/j.issn.1003-7985.2026.02.006

Synchrotron radiation sources, high-precision electronics factories, and other facilities impose extremely stringent requirements on controlling ground microvibrations. In areas near these facilities, highways are inevitably used for the transportation of goods. However, the vehicles traveling on these roads generate significant ground vibrations, which can disrupt the normal operations of precision equipment. Obtaining accurate highway traffic load data is a critical prerequisite for the prediction of traffic-induced ground vibrations and the design of microvibration control measures in synchrotron radiation sources and high-precision electronics facilities. The most common direct approaches for obtaining highway traffic loads are static weighing and dynamic weigh-in-motion methods, both of which rely on on-site measurements. However, because of the limitations of the force sensors used in these on-site weighing systems and the complex and highly variable field environments, directly measuring highway traffic loads remains technically demanding and economically challenging[1]. Therefore, in many practical applications, traffic loads are often estimated using indirect methods.

Highway traffic load inversion is categorized as the second type of inverse problem in structural dynamics, where the unknown loads are inferred from the vibration response of the structure under dynamic loads and its system parameters[2]. On this basis, researchers have proposed various indirect methods for calculating structural dynamic loads using measured response data[3-5]. These studies indicated that the attenuation laws of vibration responses to traffic loads vary depending on the driving conditions of different vehicles and the characteristics of the site soil.

In terms of frequency-domain-based load inversion methods, Peng et al.[6] used a matrix-regularization approach to simplify multiple moving loads in the spatial domain to a certain number of equivalent loads. However, this method resulted in insufficient inversion accuracy because it did not use actual load data. When testing the general traffic induction force inversion algorithm by solving the inverse problem, Sun et al.[7] used Gaussian white noise to approximate the highway traffic load effects caused by road surface irregularities. However, this method required the establishment of a complex time-domain regularization model based on Bayesian inference, and it was difficult for the inversion results to reflect the characteristics of specific sites. During on-site vibration testing, the measured response included both the usual environmental microvibration (UEM) and the actual vibration response caused by vehicles. Our field measurements showed that directly using the measured response without removing the environmental microvibration could introduce errors exceeding 20% in the recon-

Received 2025-08-01, **Revised** 2025-11-27.

Biography: XING Yunlin (1987—), male, doctor, professorate senior engineer, xingyunlin@sdic.com.cn.

Foundation item: The National Key Research and Development Program of China (No. 2023YFF0616500).

Citation: XING Yunlin, ZENG Xianhong, WU Han, et al. Improved inversion of highway traffic loads by eliminating usual environmental microvibrations[J]. Journal of Southeast University (English Edition), 2026, 42(2): 198-205. DOI: 10.3969/j.issn.1003-7985.2026.02.006.

structed response spectra. Liao et al. [1] proposed a load inversion method based on fiber Bragg grating sensors and backpropagation neural networks. This method did not explicitly treat UEM and still reported an average inversion error of 9.43%.

The frequency-domain spectral-matrix framework for random dynamic load identification based on frequency response functions (FRFs) was established[8]. Our method followed this paradigm and augmented it with microvibration removal before applying the inverse pseudo-excitation method (IPEM).

In summary, many existing highway traffic load-inversion methods either fail to explicitly address the UEM present in field responses or rely on complex vehicle-road or data-driven models. These limitations motivate the development of a more accurate and engineering-oriented inversion method that explicitly removes site microvibration and is adapted to local soil characteristics.

This study addresses the above issues by combining IPEM with UEM removal to obtain load inversions from real vibration response data. This method avoids the need for complex vehicle-road modeling and can be directly applied to engineering scenarios, providing a new solution for load inversion in microvibration-sensitive sites. This study uses a synchrotron radiation source engineering project as a case study to validate the effectiveness of the proposed method. This study analyzes the characteristics of UEM and its interference mechanism on vibration measurements, develops an improved IPEM that removes UEM from measured spectra and uses finite-element-derived FRFs to invert the responses for the load spectrum, and validates the method through field measurements at a synchrotron facility, where the relative error is reduced from 21.15% to 6.82%.

1 Impact of UEM

UEM refers to persistent small ground vibrations caused by natural or human factors, mainly comprising short-period and long-period components[9]. It is also a smooth stochastic process[10]. UEM activity originates from natural phenomena, such as ocean waves, minor earthquakes, and the atmosphere, as well as human activities in distant locations. For example, ocean-wave impacts on coastlines and interactions between water bodies and the seabed generate energy that propagates into the continental interior and onto the ground surface in the form of seismic surface waves (e.g., Rayleigh waves). Human activities include distant industrial production, construction, and mechanical operations. UEM is constantly present, even when vehicles pass by.

The frequency range of UEM is relatively wide, typically ranging from 0.001 to 10 Hz[11]. This falls within the frequency range of ground vibrations caused by traffic loads, and the vibration amplitudes are similar. For example, the vibration amplitudes of medium-distance traffic range from 0.1 to 20 μm/s, whereas those of ground vibrations caused by UEM typically range from 0.1 to 10 μm/s. Therefore, it is particularly important to remove the UEM before traffic load inversion[12]. Similarly, the dominant role of vehicle-road coupled vibrations and road surface smoothness in the ground and vehicle interior responses has been quantitatively verified in the latest bridge comfort studies[13].

2 Improved IPEM

2.1 IPEM

IPEM is applicable to load inversion in systems with deterministic structures. Recent work on the inverse finite element method and parametric inversion has also shown that inverse reconstruction combined with a measured strain field can significantly improve recognition accuracy[12]. The pseudoexcitation method was proposed by Zhi et al. [14], who then reversed this method to create IPEM. IPEM was then applied in rail transit.

A deterministic structure refers to a system whose parameters and characteristics can be described by deterministic quantities—that is, all influencing factors of the system are known, and the system's behavior and response can be predicted through precise mathematical models. Compacted soil typically exhibits deterministic structural characteristics[11]. Accordingly, the traffic load on the soil can be accurately inverted using IPEM.

One of the key advantages of IPEM is its ability to invert the time-domain and spatial-domain characteristics of highway traffic loads at different frequencies, thereby obtaining the attenuation of site vibration responses as a function of distance. For deterministic soil structures, on the basis of the theoretical framework of linear time-invariant systems, the frequency response function matrix of the system is constructed to establish a quantitative relationship between the traffic load and vibration response spectra. The vibration responses measured in site vibration tests include those caused by traffic loads and UEM inherent to the site itself. The vibration responses of UEM are not significantly different from those caused by traffic loads, making it a major interference factor in field tests.

Assuming that the soil is a linear time-invariant system, the relationship between the random vibration signal input and the output can be expressed as follows:

$$\boldsymbol{S}_{xx}(\omega) = \boldsymbol{H}(\omega)^{*}\boldsymbol{S}_{ff}(\omega)[\boldsymbol{H}(\omega)]^{\mathrm{H}} \tag{1}$$

where $\boldsymbol{S}_{xx}(\omega)$ is the response power spectral density (PSD) matrix at the measurement points, $\boldsymbol{S}_{ff}(\omega)$ is the excitation PSD matrix of the random vehicle loads, $\boldsymbol{H}(\omega)$ is the frequency response function matrix of the soil-structure system, and $[\cdot]^{\mathrm{H}}$ denotes the conjugate transpose.

In the field tests, the measured vibration response of the soil includes both the vehicle-induced vibration and the UEM of the site. Letting $\boldsymbol{y}_{\mathrm{v}}(t)$ denote the vehicle-induced component and $\boldsymbol{y}_{\mathrm{m}}(t)$ denote the UEM component of the response at the measurement points, the total measured response can then be written as

$$\boldsymbol{y}(t)=\boldsymbol{y}_{\mathrm{v}}(t)+\boldsymbol{y}_{\mathrm{m}}(t) \tag{2}$$

According to the definition of the PSD of the sum of two random processes, the PSD matrix of the measured response can be expressed as

$$\boldsymbol{S}_{yy}(\omega)=\boldsymbol{S}_{yy}^{\mathrm{v}}(\omega)+\boldsymbol{S}_{yy}^{\mathrm{m}}(\omega)+\boldsymbol{S}_{\mathrm{vm}}(\omega)+\boldsymbol{S}_{\mathrm{mv}}(\omega) \tag{3}$$

where $\boldsymbol{S}_{yy}^{\mathrm{v}}(\omega)$ is the PSD matrix of the vehicle-induced vibration response, $\boldsymbol{S}_{yy}^{\mathrm{m}}(\omega)$ is the PSD matrix of the UEM, and $\boldsymbol{S}_{\mathrm{vm}}(\omega)$ and $\boldsymbol{S}_{\mathrm{mv}}(\omega)$ are the cross-power spectral density matrices between $\boldsymbol{y}_{\mathrm{v}}(t)$ and $\boldsymbol{y}_{\mathrm{m}}(t)$.

Because the vehicle-induced vibration and the inherent microvibration arise from different physical mechanisms, they are assumed to be statistically independent. Consequently, their cross-power spectral densities vanish:

$$\boldsymbol{S}_{\mathrm{vm}}(\omega)=\boldsymbol{S}_{\mathrm{mv}}(\omega)=\mathbf{0} \tag{4}$$

Then, Eq. (3) is reduced to

$$\boldsymbol{S}_{yy}(\omega)=\boldsymbol{S}_{yy}^{\mathrm{v}}(\omega)+\boldsymbol{S}_{yy}^{\mathrm{m}}(\omega) \tag{5}$$

Assuming that the load application location is known and the dynamic response of the system is obtained from field testing, the identification of the steady-state random loads based on IPEM proceeds as follows.

The dynamic response of the soil tested on-site includes vehicle-induced vibration responses and the soil's own UEM. Therefore, the PSD can be expressed as

$$\boldsymbol{S}_{cc}(\omega)=\boldsymbol{S}_{yy}(\omega)+\boldsymbol{S}_{aa}(\omega)+2\mathrm{Re}(\boldsymbol{S}_{ya}(\omega)) \tag{6}$$

where $\boldsymbol{S}_{cc}(\omega)$ is the PSD of the vibration response at the measurement points, $\boldsymbol{S}_{yy}(\omega)$ is the PSD of the vehicle-induced vibration response, $\boldsymbol{S}_{aa}(\omega)$ is the PSD of the UEM, and $\mathrm{Re}(\boldsymbol{S}_{ya}(\omega))$ is the real part of the cross-spectrum between the vibration responses caused by the vehicle and the UEM. The vehicle-induced vibration response is independent of the UEMs of the soil itself; thus, their mutual spectrum is zero.

Eq. (6) can be rewritten as

$$\begin{aligned}\boldsymbol{S}_{cc}(\omega)&=\boldsymbol{S}_{yy}(\omega)+\boldsymbol{S}_{aa}(\omega)=\\&\boldsymbol{H}(\omega)\boldsymbol{S}_{ff}(\omega)[\boldsymbol{H}(\omega)]^{\mathrm{H}}+\boldsymbol{S}_{aa}(\omega)\end{aligned} \tag{7}$$

Spectral decomposition is performed on the response PSD matrix $\boldsymbol{S}_{yy}(\omega)$:

$$\boldsymbol{S}_{yy}(\omega)=\sum_{i=1}^{r}\boldsymbol{b}_i(\omega)[\boldsymbol{b}_i(\omega)]^{\mathrm{H}} \tag{8}$$

where r is the rank of the response PSD matrix.

The spectral decomposition of the UEM PSD matrix $\boldsymbol{S}_{aa}(\omega)$ is then performed:

$$\begin{aligned}\boldsymbol{S}_{aa}(\omega)&=\sum_{i=1}^{r}\boldsymbol{a}_i(\omega)[\boldsymbol{a}_i(\omega)]^{\mathrm{H}}=\boldsymbol{S}_{cc}(\omega)-\\&\sum_{i=1}^{r}\boldsymbol{b}_i(\omega)[\boldsymbol{b}_i(\omega)]^{\mathrm{H}}\end{aligned} \tag{9}$$

The virtual responses are constructed as follows:

$$\boldsymbol{y}_i(\omega)=\boldsymbol{b}_i(\omega)\mathrm{e}^{\mathrm{j}\omega t} \tag{10}$$

Assuming that the vehicle-induced virtual response $\boldsymbol{y}_i(\omega)$ is generated by the vehicle's virtual stimulus $\boldsymbol{x}_i(\omega)=\boldsymbol{\alpha}_i(\omega)\mathrm{e}^{\mathrm{j}\omega t}$, then

$$\boldsymbol{a}_i(\omega)=[\boldsymbol{H}(\omega)]^{+}\boldsymbol{b}_i(\omega)=[\boldsymbol{H}(\omega)]^{+}(\boldsymbol{c}_i(\omega)-\boldsymbol{a}_i(\omega)) \tag{11}$$

where the superscript symbol "+" denotes the generalized inverse operation of the matrix.

The excitation PSD matrix is identified as

$$\boldsymbol{S}_{xx}(\omega)=\sum_{i=1}^{r}\boldsymbol{a}_i(\omega)[\boldsymbol{a}_i(\omega)]^{\mathrm{H}} \tag{12}$$

According to Eq. (6), the traffic load spectrum can be derived using IPEM:

$$\boldsymbol{F}(\omega)=[\boldsymbol{H}(\omega)]^{+}(\boldsymbol{X}(\omega)-\boldsymbol{A}(\omega)) \tag{13}$$

According to Eq. (6), if the effects of the UEM are ignored, the measured vibration response is expressed, affecting the accuracy of highway traffic loads.

2.2 Frequency response function matrix

Establishing a finite element model of soil mass is a critical step in studying ground soil vibration responses and frequency response function matrices caused by highway traffic loads. When defining soil properties, precise settings based on measured and inverted soil data must be utilized. Key parameters, such as soil layer thickness, shear wave velocity, Poisson's ratio, density, and damping ratio, are obtained through field geological surveys and soil dynamic parameter inversion based on continuous microtremors[15]. These measured data provide important foundational support for the subsequent establishment of soil finite element models, ensuring their accuracy.

Because the finite element model has finite dimensions while the actual soil body is infinite, viscoelastic boundary conditions must be applied at the boundaries of the soil model to simulate the characteristics of an infinite soil body[16]. A unit force is applied at the center of the model to facilitate harmonic response analysis and thereby obtain the frequency-domain characteristics of the vibration response at different distances from the soil surface under a unit force.

By simulating the vibration response at various points on the soil surface, the site attenuation characteristics of the soil simulation analysis can be determined. The frequency range and resolution of the harmonic response analysis should align with those of the measured site vibration response $\boldsymbol{X}_i(\omega)$ to ensure the reliability of the analysis results. In engineering applications, such as synchrotron radiation sources and high-precision electronics factories, the primary focus is on the vibration effects caused by traffic on the soil surface below 100 Hz[17]. In this respect, Zhang et al. [18] found that the ground-borne vibrations caused by road vehicles decreased with increasing propagation distance, peaking near 10 Hz. Therefore, the frequency range for the harmonic response analysis was set to 0-100 Hz, with a frequency resolution of 0.25 Hz, to balance analysis accuracy and computational efficiency. Finally, the vibration amplitude and phase at each point on the soil surface were output—combined with the distance from the point where the unit force was applied and the magnitude of the vibration displacement—to form the decay law of the simulated soil vibration response and derive the soil frequency response function.

2.3 Improved method for eliminating the influence of UEMs

During on-site testing, three measurement points were arranged perpendicular to the road traffic lanes to be tested, as shown in Fig. 1.

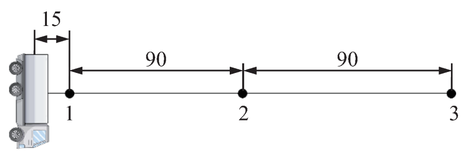

Fig. 1 Layout of the measurement points (unit: m)

The three measurement points had their own specific functions:

(1) Measurement point 1 served as a time control point primarily responsible for precisely recording the exact time when a vehicle passed through it, providing a time reference for the subsequent data analysis.

(2) Measurement point 2 served as a load inversion measurement point. Its data were directly used for traffic load inversion calculations, making it the core data source for the load inversion analysis.

(3) Measurement point 3 served as a response comparison point. Its primary function was to validate the load results obtained from inversion. By comparing the measured vibration response with that calculated from the load inversion, the accuracy and reliability of the load inversion results were assessed.

This measurement point layout ensured the specificity of each measurement point's function while cross-validating the data through multipoint collaboration, providing a reliable data foundation for subsequent load inversion and analysis.

The vibration response $\boldsymbol{x}_i(t)$ was collected for the vehicle operating conditions, whereas the site microvibration $\boldsymbol{a}_i(t), i = 1, 2, 3$ was collected for the non-vehicle operating conditions. Fast Fourier transforms and self-spectrum analyses were performed on both, including the frequency-domain amplitude and phase. Then, the PSD of the true vibration response was obtained after removing the microvibration according to Eq. (6).

2.4 Inversion accuracy quantification method

To scientifically evaluate the accuracy of the proposed traffic load inversion method, the following quantitative verification process was established:

Step 1 Measurement point 1 was used to extract effective vibration signal samples from the vibration response data for various operating conditions in the time domain.

Step 2 A finite element model of the soil was established, and harmonic response analysis was performed to calculate the frequency response function $H(\omega)$.

Step 3 Load inversion calculations were performed using data from measurement point 2 to obtain the inverted load PSD. The calculation results are recorded as $\boldsymbol{S}_{ff3}$.

Step 4 The inverted load PSD $\boldsymbol{S}_{ff3}$ was substituted into Eq. (2) to calculate the PSD. The vibration response PSD of measurement point 3 was reconstructed, the site's microtremor response spectrum was superimposed, the comprehensive vibration response PSD $\boldsymbol{S}_{yy4}$ was obtained, and the 1/3-octave band $\boldsymbol{X}_{f4}$ was calculated.

Step 5 For the error quantification analysis, the composite vibration response 1/3-octave spectrum $\boldsymbol{X}_{f4}$ obtained in Step 4 and the actual vibration response 1/3-octave spectrum $\boldsymbol{X}_3$ were used to calculate the relative error, expressed as

$$e = \frac{\| \boldsymbol{X}_{f4} - \boldsymbol{X}_3 \|_1}{\| \boldsymbol{X}_3 \|_1} \times 100\% \tag{14}$$

The smaller the error e, the higher the load inversion accuracy and the more accurate the reconstruction of the vibration response characteristics caused by the actual highway traffic load.

This quantitative method utilized the cross-validation of multiple sets of measurement points to form a closed-loop verification system consisting of "actual measurement-modeling-inversion-reconstruction-error assessment," effectively ensuring the reliability of the load inversion results.

3 Engineering Applications

3.1 Site conditions

The selected test site was that of a synchrotron radiation source project. A heavily trafficked road was located approximately 210 m south of the site. Because the highway traffic loads generated by vehicle movement might be transmitted through soil vibrations and have adverse effects on the site, a systematic assessment of the load impacts was conducted by simulating real-world road traffic conditions.

To accurately test the soil vibration response caused by traffic loads, three measurement points were set up at distances of 15, 90, and 180 m from the centerline of the roadway and perpendicular to the direction of traffic flow. The specific layout of the measurement points is shown in Fig. 1.

The test conditions were divided into two categories: vehicle passage and UEM. In the vehicle passage conditions, a 30-t dump truck was used as the test vehicle, traveling at a constant speed of 40 km/h across the traffic road. During the constant condition test, within a 300 m radius of the measurement point, no vehicles were seen traveling, and no significant vibration sources affected the measurement point.

The vehicle type and speed for the vehicle passage conditions were chosen to simulate common driving conditions of heavy vehicles in actual traffic to accurately reflect the impact of highway traffic loads on ground soil vibrations. To ensure the accuracy and stability of the vibration response data, loose soil on the surface of the measurement points was removed to reduce interference and ensure good contact between the sensors and the soil. Multiple long steel nails were used to securely attach the iron plate to the hard soil layer, ensuring the stability of sensor installation. Each measurement point was equipped with a data acquisition unit and a 941B-type high-sensitivity magnetoelectric sensor, which was installed on the steel plate to precisely collect the time-domain data for the vertical soil vibration response ($x_i(t)$, $i = 1, 2, 3$). The data acquisition units at each measurement point were synchronized via GPS timing. This configuration effectively ensured the stability and accuracy of the data acquisition process. On the basis of Nyquist's theorem, the sampling frequency for the vibration response was set to 1 024 Hz. This frequency setting ensured the adequate sampling of the vibration signal and the accurate capture of vibration characteristics caused by traffic loads while avoiding aliasing during data acquisition.

To analyze the impact of UEMs on load inversion, the time-domain vibration response data for the two types of operating conditions were obtained from measurement point 2 using the aforementioned layout and data acquisition methods. As shown in Fig. 2, the time histories of the vibration velocity at measurement point 3 were compared for two conditions: a traffic-free interval (shown in red) as the UEM and an isolated vehicle pass by (shown in blue). The background remained near zero, whereas the pass-by exhibited much larger, time-localized amplitudes. The vibration response was primarily caused by vehicles traveling on uneven road surfaces, vehicle acceleration and deceleration, and interactions between vehicle wheels and the ground. This resulted in the vehicles moving up and down at different frequencies and vibration amplitudes, thereby causing vibration transmission to the ground and reflecting vibration changes induced by the passing vehicles. A comparative analysis indicated that the vibration response under UEM conditions was similar to that under vehicle passage conditions. Therefore, when measured response data are directly used for the highway traffic load inversion, the influence of the UEM could significantly interfere with the inversion results, affecting the accuracy and reliability of the load inversion.

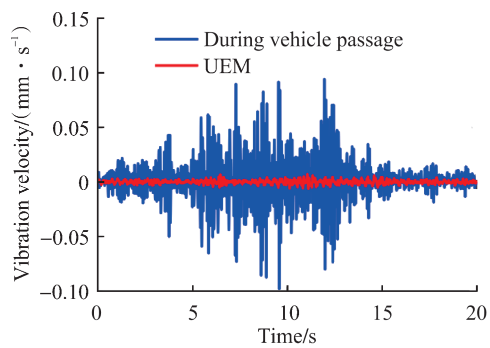

Fig. 2 Vibration response comparison diagram

3.2 Model establishment and simulation analysis

The dynamic parameters of the soil were obtained using the data provided in the geological survey report and the inversion method for the soil's dynamic parameters based on continuous microtremors. The soil profile was then simulated and modeled using the finite element software Ansys. The detailed soil dynamic parameters are shown in Table 1, which include the damping ratio, thickness, shear wave velocity, Poisson's ratio, Rayleigh wave velocity, and elastic modulus of the soil layer. These parameters were used to construct the finite element model.

Table 1 Dynamic parameters of the soil

Geotechnical name	Thickness/m	Shear wave velocity/(m·s^{-1})	Damping ratio	Density/(t·m^{-3})
Fill soil	1.82	130	0.035	1.9
Clay	11.2	280	0.03	2.0
Strongly weathered mudstone sandstone	3.1	425	0.03	2.2
Weathered mudstone sandstone	40	600	0.03	2.2

The soil's dynamic properties were determined using key parameters such as the shear modulus G, elastic modulus E, and Rayleigh wave velocity V_R. According to the elasticity theory, the relationship between the shear wave velocity V_s and the shear modulus G can be expressed as

$$G = \rho V_s^2 \tag{15}$$

where ρ is the soil density. This equation indicates that V_s directly characterizes the shear stiffness of the soil. V_R, as the main vibration carrier, has propagation characteristics controlled by V_s and Poisson's ratio ν, satisfying the following approximate relationship:

$$V_R \approx \frac{0.862 + 1.14\nu}{1 + \nu} V_s \tag{16}$$

The elastic modulus E can be derived from G and ν:

$$E = 2G(1 + \nu) \tag{17}$$

When establishing a finite element model using Ansys, the G values of each soil layer were calculated from ρ and V_s, and combined with ν to determine E and V_R. This ensured that the model had a clearer physical meaning. Considering the difference between the finite nature of the finite element model and the infinite nature of the actual soil, viscoelastic boundary conditions were applied to the boundaries of the soil model. These boundary conditions effectively simulated the characteristics of an infinite soil body, thereby improving the simulation accuracy of the model[16]. A vertical downward unit point load was set at the top of the model to simulate traffic loads.

Harmonic response analysis was employed in this study to evaluate the vibration response characteristics of the soil at different frequencies. The analysis frequency ranged from 0 to 100 Hz, with a frequency interval of 0.25 Hz, to ensure the comprehensive capture of the vibration effects from the low-frequency to mid-frequency ranges. The full method was used to solve the response problem, and a sparse direct equation solver was employed to improve the computational efficiency. The final output included the vertical vibration amplitude and phase information at key points on the top of the soil model, denoted as $\boldsymbol{H}(\omega)$.

3.3 Load inversion results based on the improved IPEM

Fig. 3 compares the load spectra identified from two inputs: the blue curve was obtained from the raw measured vibration response, whereas the red curve was obtained from the true response after subtracting the UEM. This demonstrates that load identification was necessary after eliminating the UEM.

The identified traffic loads were reconstructed to obtain the theoretical vibration response, which was then compared with the measured vibration response. The results are shown in Fig. 4, where curve A represents the frequency band energy distribution of the measured vibration velocity under vehicle passage conditions, curve B represents the theoretical response reconstructed from the measured response without removing the UEM, and curve C represents the comprehensive response obtained by superimposing the UEM on the theoretical response reconstructed from the measured response without the UEM.

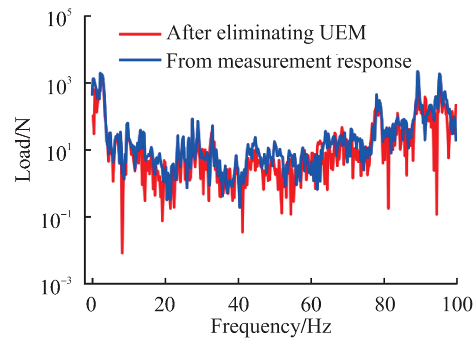

Fig. 3 Load comparison diagram

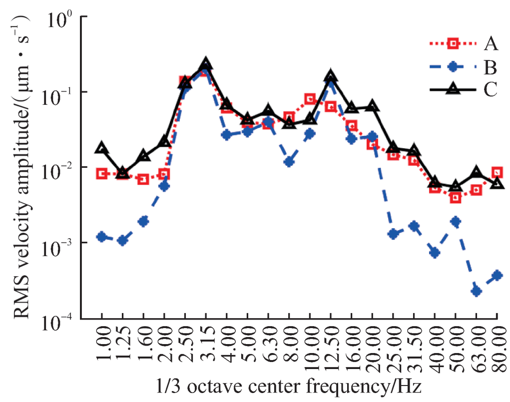

Fig. 4 1/3 octave plot of response comparison

The frequencies of the identified highway traffic load vibration response mainly ranged from 0 to 20 Hz, which had the largest contribution. Therefore, the analysis focused on the relative error analysis in the three ranges of 0-100, 0-20, and 20-100 Hz.

An error quantification analysis was performed according to Eq. (10), and the results are shown in Table 2. Within the frequency range of 0-100 Hz, the relative error between curves A and B was 21.15%, whereas that between curves A and C was significantly reduced to 6.82% (a reduction of 14.33%). UEM interference could cause systematic deviations in the load inversion (with errors exceeding 15%). By removing the UEM to obtain the true vibration response, the load identification error could be controlled within a 7% range.

Within the frequency range of 0-20 Hz, the relative error between curves A and B was 10.44%, whereas that between curves A and C was significantly reduced to 9.17% (a reduction of 1.27%). Within the frequency

Table 2 Comparison for error quantification

Frequency range/Hz	Relative error of the traditional method's curves A and B/%	Relative error of the improved method's curves A and C/%	Error reduction/%
0-100	21.15	6.82	14.33
0-20	10.44	9.17	1.27
20-100	22.36	6.38	15.98

range of 20-100 Hz, the relative error between curves A and B was 22.36%, whereas that between curves A and C was significantly reduced to 6.38% (a reduction of 15.98%).

To explain the differences in the results shown in Fig. 4, the spectrum diagrams for the UEM and vehicle passage are compared in Fig. 5. When the frequency was between 2 and 15 Hz, the vibration response when a vehicle passed by was much larger than that of the UEM. Therefore, when performing load inversion in this frequency range, the influence of the UEM was relatively small. However, in the frequency ranges of 1-2 and 15-100 Hz, the vibration response when a vehicle passed by was essentially the same as that of the UEM. In this case, the UEM must be eliminated. If it were not eliminated, a large error would occur.

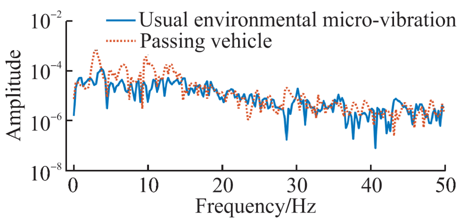

Fig. 5 Frequency spectrum comparison

4 Conclusions

This study combined the traffic load inversion results from a certain synchrotron radiation project site to analyze the impact of site-specific microtremors on load inversion. The feasibility and effectiveness of the highway traffic load inversion method were verified using IPEM with microtremor removal, leading to the following conclusions:

(1) By removing UEMs, the improved method achieved relative error reductions of 14.33% in the frequency range of 0-100 Hz and 15.98% in the frequency range of 20-100 Hz, verifying its accuracy under complex conditions.

(2) The method presented in this study yielded a relatively accurate identification of the traffic load spectrum in the frequency range of 2-15 Hz, which was the dominant band for the ground microvibration at the studied site.

(3) The proposed load inversion method provides a high-precision, low-complexity solution with significant engineering application value.

References

[1] LIAO M H, LIANG S, LUO R, et al. The moving load identification method on asphalt roads based on the BP neural network and FBG sensor monitoring [J]. Construction and Building Materials, 2023, 378: 131216.

[2] ZHU X Q, LAW S S. Recent developments in inverse problems of vehicle-bridge interaction dynamics [J]. Journal of Civil Structural Health Monitoring, 2016, 6(1): 107-128.

[3] LIU J, SUN X S, HAN X, et al. Dynamic load identification for stochastic structures based on Gegenbauer polynomial approximation and regularization method[J]. Mechanical Systems and Signal Processing, 2015, 56/57: 35-54.

[4] LI X W, ZHAO H T, CHEN Z, et al. Force identification based on a comprehensive approach combining Taylor formula and acceleration transmissibility[J]. Inverse Problems in Science and Engineering, 2018, 26(11): 1612-1632.

[5] PAN C D, YU L. Identification of external forces via truncated response sparse decomposition under unknown initial conditions[J]. Advances in Structural Engineering, 2019, 22(15): 3161-3175.

[6] PENG S X, PAN C D, CHEN X D, et al. Applying matrix regularization to identification of traffic-induced equivalent loads and multi-vehicle weight on beam-like bridge[J]. Journal of Sound and Vibration, 2024, 590: 118592.

[7] SUN H, BÜYÜKÖZTÜRK O. Identification of traffic-induced nodal excitations of truss bridges through heterogeneous data fusion[J]. Smart Materials and Structures, 2015, 24(7): 075032.

[8] WU S Q, HE Z H, YIN J, et al. Identification of annularly distributed random dynamic load between satellite and rocket in frequency domain[J]. Journal of Southeast University (Natural Science Edition), 2022, 52(5): 825-832. (in Chinese)

[9] GAO S C, XIE M W, ZHANG X Y, et al. Research on vibration characteristics of cantilevered dangerous rock mass[J]. Mining Research and Development, 2023, 43(6): 147-153. (in Chinese)

[10] ZHANG X, SUN W B, ZHANG Q X, et al. Study on the application of passive seismic interferometric imaging technology in the detection of goaf in coalfield[J]. Geological Review, 2024, 70(5): 1899-1905. (in Chinese)

[11] ZHANG T, LI T, FENG S. Elastoplastic two-surface model for describing strain-softening behavior of saturated cohesive soils [J]. Rock and Soil Mechanics, 2022, 43(10): 2757-2767. (in Chinese)

[12] GU Y Q, CAO W Z, YUAN S F, et al. Inverse finite element method based shape reconstruction for spaceborne

antenna structures under thermal load［J］. Journal of Southeast University（Natural Science Edition）, 2024, 54(4): 997-1004.（in Chinese）
［13］FENG D M, WANG B Q, XIA Y, et al. Analysis on driving comfort of large-span girder bridges considering traffic flow load［J］. Journal of Southeast University（Natural Science Edition）, 2025, 55(2): 468-476.（in Chinese）
［14］ZHI H, GUO X L, LIN J H. Inverse virtual excitation method for stationary random vibration load identification（Ⅱ）［J］. Chinese Journal of Computational Mechanics, 1998, 15(4): 395-400.
［15］LOU Y, XING Y L, LÜ Z C, et al. Inversion method for soil dynamics parameters of high energy photon source［J］. Journal of Southeast University（Natural Science Edition）, 2023, 53(6): 973-978.（in Chinese）
［16］LIU J B, GU Y, DU Y X. Consistent viscous-spring artificial boundaries and viscous-spring boundary elements［J］. Chinese Journal of Geotechnical Engineering, 2006, 28(9): 1070-1075.（in Chinese）
［17］DUCARNE L, AINALIS D, KOUROUSSIS G. Assessing the ground vibrations produced by a heavy vehicle traversing a traffic obstacle［J］. Science of the Total Environment, 2018, 612: 1568-1576.
［18］ZHANG Z J, LI X Z, ZHANG X, et al. Measurements and evaluation of road traffic-induced micro-vibration in a workshop equipped with precision instruments［J］. Buildings, 2024, 14(4): 1142.

消除常时微动的改进公路交通荷载反演

邢云林[1]，曾宪鸿[2]，吴晗[3]，娄宇[1]

（1.中国电子工程设计院股份有限公司，北京 100142；2.五邑大学轨道交通学院，江门 529020；
3.中国科学院力学研究所，北京 100190）

摘要：常时微动会对现场实测的交通引起的振动响应造成影响，从而导致公路交通荷载反演结果存在较大误差。为此，本文提出了一种消除常时微动的改进公路交通荷载反演方法，该方法与逆虚拟激励法相结合，用于公路交通荷载的反演。通过频域变换将场地实测地面振动响应中的常时微动分离出来，从而获得由交通荷载引起的真实振动响应。随后，采用有限元仿真技术求取频率响应函数。最后，通过对频率响应函数矩阵进行矩阵求逆运算，反演得到交通荷载谱。以某同步辐射光源工程为例，利用反演得到的交通荷载谱计算测点处的振动响应，并与现场实测结果进行对比。结果表明，相对误差由21.15%降低至6.82%，验证了所提方法的有效性。该方法避免了复杂的车–路耦合分析，为微振动敏感场地的荷载反演提供了一种可靠的技术手段。

关键词：逆虚拟激励法；常时微动；公路交通荷载；微振动敏感场地

中图分类号：TU435